

A Multiband Study of the Optically Dark GRB 051028

Yuji URATA,¹ Kui-Yun HUANG,² Ping-Hung KUO,² Wing-Huen IP,² Yulei QIU,³
Keisuke MASUNO,¹ Makoto TASHIRO,¹ Keiichi ABE,¹ Kaori ONDA,¹ Natsuki KODAKA,¹
Makoto KUWAHARA,^{4,5} Toru TAMAGAWA,⁵ Fumihiko USUI,⁶ Kunihito IOKA,⁷
Yi-Hsi LEE,² Jianyan WEI,³ Jinsong DENG,³ Weikang ZHENG,³ and Kazuo MAKISHIMA^{8,4}

¹*Department of Physics, Saitama University, 255 Shimo-Okubo, Sakura-ku, Saitama 338-8570*

²*Institute of Astronomy, National Central University, Chung-Li 32054, Taiwan*

³*National Astronomical Observatories, Chinese Academy of Sciences, Beijing 100012, China*

⁴*Tokyo University of Science, 1-3 Kagurazaka, Shinjuku-ku, Tokyo 162-8601*

⁵*RIKEN (Institute of Physical and Chemical Research), 2-1 Hirosawa, Wako, Saitama 351-0198*

⁶*Institute of Space and Astronomical Science, Japan Aerospace Exploration Agency, Sagami-hara, Kanagawa 229-8510*

⁷*Department of Physics, Kyoto University, Kitashirakawa, Sakyo-ku, Kyoto 606-8602*

⁸*Department of Physics, The University of Tokyo, 7-3-1 Hongo, Bunkyo-ku, Tokyo 113-0033*

urata@crystal.heal.phy.saitama-u.ac.jp

(Received 2006 October 17; accepted 2007 May 31)

Abstract

Observations were made of the optical afterglow of GRB 051028 with the Lulin observatory 1.0 m telescope and the Wide-Field Telescope for GRB Early Timing (WIDGET) robotic telescope system. *R*-band photometric data were obtained on 2005 October 28 (UT), or 0.095–0.180 d after the burst. There is a possible plateau in the optical light curve around 0.1 d after the burst; the afterglow of GRB 051028 resembles optically bright afterglows (e.g., GRB 041006, GRB 050319, GRB 060605) in shape of the light curve, but not in brightness. The brightness of the GRB 051028 afterglow is 3 mag fainter than that of one of the dark events, GRB 020124. Optically dark GRBs have been attributed to dust extinction within the host galaxy or a high redshift. However, a spectrum analysis of the X-rays implies that there is no significant absorption by the host galaxy. Furthermore, according to a theoretical calculation of the Ly α absorption to find the limit of the GRB 051028's redshift, the expected *R*-band absorption is not high enough to explain the darkness of the afterglow. The present results disfavor either the high-redshift hypothesis or the high-extinction scenario for optically dark bursts; rather, they are consistent with the possibility that the brightness of the optical afterglow is intrinsically dark.

Key words: gamma-rays: bursts: optical afterglow — techniques: photometric

1. Introduction

In recent years, BeppoSAX and HETE-2 have provided quick positional information on a number of gamma-ray bursts (GRBs) with a typical positional accuracy of $\sim 10'$, which has led to rapid follow-up observations in the optical and near-infrared frequencies. The Swift satellite has opened the door to making high-sensitivity X-ray afterglow observations with an X-ray telescope in the early stage of afterglows. This revealed that almost all of the GRBs had an X-ray afterglow; the positions of the GRBs could be measured to a precision of $10''$. Nevertheless, the afterglow associated with about half of the promptly localized GRBs was either very faint (> 23 mag 1 d after the burst, Fynbo et al. 2001), or nonexistent (Lamb et al. 2003). Such events are broadly termed “optically dark GRBs”. To be more precise, in this paper we define a GRB to be “optically dark” if its optical afterglow is fainter than 23 mag at 1 d after a burst. Typical optically dark GRBs include GRB 030115 and GRB 021211. The afterglow of GRB 030115 was extremely red; although a near-infrared counterpart with $K \sim 19$ was detected 1 d after the burst, no optical afterglow brighter than 20 mag was detected, even at 0.1 d. In the case of GRB 021211, the afterglow showed a rapid

decay until around 0.1 d, fading to > 22 mag by the next day.

The observations of the afterglow of a GRB via X-rays through radio frequencies can be interpreted by the fireball models. In general, a shock produced by interaction of relativistic ejecta with the circumburst medium will lead to the radiation of broadband synchrotron emission. Assuming this widely accepted hypothesis to be true, there are three possible explanations for optically dark GRBs: (1) They have such high redshifts ($z > 5$) that optical afterglows suffer from strong Lyman absorption (Heise 2001); (2) The optical afterglow has been extinguished by dust in the vicinity of the GRB or in the star-forming region in which the GRB occurs (Piro et al. 2002; Klose et al. 2003); (3) The optical afterglow exhibits rapid decay from a very early phase, such as has been reported for GRB 020124 and GRB 021211 (Berger et al. 2002; Yamazaki et al. 2003; Crew et al. 2003).

In this paper we present an analysis of the optical and X-ray afterglow of an optically dark event, GRB 051028. At 13:36:01.47 UT on 2005 October 28, the HETE-2 French Gamma Telescope (FREGATE) and Wide Field X-Ray Monitor (WXM) (Shirasaki et al. 2003) instruments detected a bright GRB (Hurley et al. 2005). The burst triggered the operation of FREGATE in the 30–400 keV energy band.

The burst duration (T90)¹ was 16 s in both the 30–400 keV band and the 7–30 keV band. A ground analysis of the WXM data found a 90% confidence error region measuring $33' \times 18'$ with corners at the following coordinates (J2000.0): $\alpha = 01^{\text{h}}50^{\text{m}}19^{\text{s}}.6$, $\delta = +47^{\circ}41'06''$; $\alpha = 01^{\text{h}}47^{\text{m}}01^{\text{s}}.1$, $\delta = +47^{\circ}38'02''$; $\alpha = 01^{\text{h}}46^{\text{m}}58^{\text{s}}.3$, $\delta = +47^{\circ}55'55''$; and $\alpha = 01^{\text{h}}50^{\text{m}}17^{\text{s}}.5$, $\delta = +47^{\circ}58'58''$. The 30–400 keV fluence of GRB 051028 is $6 \times 10^{-6} \text{ erg cm}^{-2}$; the 2–30 keV fluence is $6 \times 10^{-7} \text{ erg cm}^{-2}$. The hardness ratio allows us to classify this burst as a classical GRB (Hurley et al. 2005). Swift XRT started to observe the field about 7.1 hr after the burst, and found the X-ray afterglow at $\alpha = 01^{\text{h}}48^{\text{m}}15^{\text{s}}.1$, $\delta = +47^{\circ}45'12''.5$ (J2000.0) with an uncertainty of $6''$ (90% containment) (Racusin et al. 2005). The optical afterglow was also reported by Jelinek et al. (2005) at coordinates of $\alpha = 01^{\text{h}}48^{\text{m}}15^{\text{s}}.01$, $\delta = +47^{\circ}45'09''.2$ (J2000.0).

2. Observations

Optical observations were made by the East-Asia GRB Follow-up Observation Network (EAFON²; Urata et al. 2005) using two kinds of telescopes.

2.1. Pre-GRB Observation with WIDGET

We observed the error region of GRB 051028 (Hurley et al. 2005) with the very wide-field camera WIDGET (Tamagawa et al. 2005). WIDGET (WIDE-field telescope for GRB Early Timing) is a robotic telescope. It monitors the HETE-2 field-of-view and can detect GRB optical flashes or possible optical precursors. The field-of-view is $62^{\circ} \times 62^{\circ}$, which covers about 80% of the HETE-2 WXM observing field. The system consists of a $2\text{k} \times 2\text{k}$ Apogee U10 CCD camera and a Canon EF 24 mm f/1.4 wide-angle lens. WIDGET has been in operation at the Akeno site (Longitude and Latitude are $138^{\circ}30'$ E and $35^{\circ}47'$ N, respectively) since 2004 June. WIDGET monitored the GRB 051028 region by repeated, unfiltered 5 s exposures taken 16.0 min and 11.2 min before the burst (Masuno et al. 2006).

2.2. Follow-up Observation at Lulin

We started optical follow-up observations using Lulin's One-meter Telescope (LOT) (Huang et al. 2005) 0.094 d after the burst (i.e., 12 min after the HETE-2 position alert). This is the fastest follow-up observation with a telescope in the 1 m class. This telescope was installed in 2002 September on the summit of Mount Lulin ($120^{\circ}52'25''$ E, $23^{\circ}28'7''$ N, H = 2862 m) in Central Taiwan by the Institute of Astronomy of National Central University. Photometric images were obtained with a PII300B CCD camera (1340×1300 pixels: 11.5×11.2 field of view). A sample is shown in figure 1. To cover the entire HETE-2 WXM error box ($33' \times 18'$), we imaged an 8-field mosaic with 300 s exposures in the *R* band. Due to the darkness and unclear variability during the early part of our observations, as shown in figure 2, we could not quickly identify the afterglow by analysis at the observing site. The obtained *R*-band data are described in table 1.

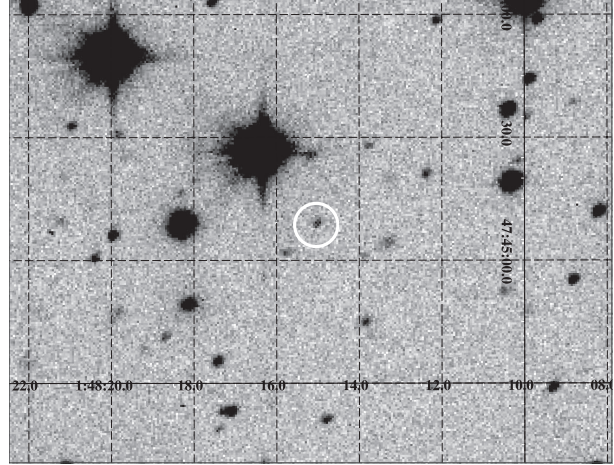


Fig. 1. *R*-band image of the GRB 051028 field obtained at the Lulin Observatory with a 300 s exposure. The circle near the center of the image indicates the afterglow.

Table 1. Lulin photometric results.

Delay (d)	Filter	Magnitude
0.095	<i>R</i>	20.77 ± 0.08
0.099	<i>R</i>	20.71 ± 0.06
0.103	<i>R</i>	20.77 ± 0.06
0.107	<i>R</i>	20.76 ± 0.06
0.111	<i>R</i>	20.88 ± 0.07
0.147	<i>R</i>	21.19 ± 0.09
0.180	<i>R</i>	21.45 ± 0.14
0.262	<i>R</i>	21.80 ± 0.13

3. Analysis and Results

3.1. WIDGET

Data reduction of the WIDGET images was performed by the standard method. Each WIDGET image taken around the GRB position was compared with nonsaturated bright stars in the Tycho-2.0 position catalog. The rms deviation around the fit to the positions of 8 reference stars was $231''$. We did not find any optical emission from the afterglow position (Jelinek et al. 2005). The $1\text{-}\sigma$ limiting magnitude of each frame derived from the Tycho-2 catalog was around $V = 10.3$ mag.

3.2. LOT

A standard routine including bias subtraction, dark subtraction, and flat-fielding corrections with appropriate calibration data was employed to process the data using IRAF. As shown in figure 1, the afterglow can clearly be seen in the *R*-band image. Flux calibrations were performed using the APPHOT package in IRAF, referring to the standard stars suggested by Henden (2005). For each data set, the one-dimensional aperture size was set to 4 times as large as the full width at half maximum of the objects. The magnitude of the error for each optical image is estimated to be $\sigma_c^2 = \sigma_{\text{ph}}^2 + \sigma_{\text{sys}}^2$, where σ_{ph} represents the photometric error for the GRB 051028 afterglow, estimated from the output of IRAF

¹ T90 is defined as the burst duration for which 90 percent of the whole counts are detected.

² (<http://cosmic.riken.jp/grb/eafon/>).

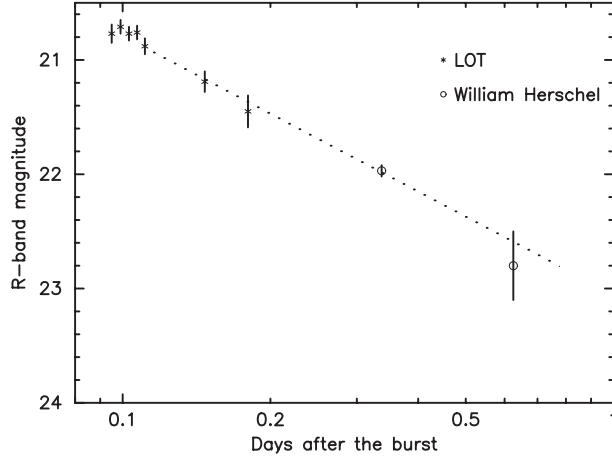


Fig. 2. *R*-band light curve based on photometry of the Lulin (LOT) photometry. The dashed line indicates the best-fit function for the light curve during the period from 0.11 to 0.63 d after the burst.

PHOT, and σ_{sys} is the photometric calibration error, estimated by comparing our instrumental errors for the 7 standard stars over the 9 frames.

Figure 2 shows the *R*-band light curve of the GRB 051028 afterglow. There is a clear plateau phase seen about 0.1 d after the burst. This early phase plateau is often seen in optically bright afterglows, such as with GRB 041006 (Urata et al. 2007a), GRB 021004 (Urata et al. 2007b), and GRB 050319 (Huang et al. 2006). Around 0.11 d after the burst, the optical afterglow started to decay. We tried to fit the decaying *R*-band light curves using as a simple power law of time t after the onset of the burst, t^α , where α is the decay index. We obtained $\alpha = -1.06 \pm 0.04$ with a reduced chi-squared (χ^2/ν) of 0.029 for $\nu = 1$. In order to better constrain the late-time (> 0.3 d) behavior of the light curve, we combined our data with the two *R_c*-band photometric points taken by the William Herschel telescope: $R = 21.97 \pm 0.05$ mag at 0.337 d, and $R = 22.8 \pm 0.3$ mag at 0.625 d (Castro-Tirado et al. 2006). We again successfully fitted the combined *R*-band light curve with a single power law, for which the decay index is -0.904 ± 0.037 with $\chi^2/\nu = 0.33$ for $\nu = 3$.

3.3. *Swift*/XRT

In order to compare the X-ray afterglow with the optical one, we also analyzed X-ray data taken by Swift X-Ray Telescope (XRT). The data for GRB 051028 were downloaded from the Swift archive and reduced by running version 0.10.3 of the `xrtpipeline` reduction script from the HEASOFT 6.0.6³ software package. However, for the four series of observations, the significance was close to $3\text{-}\sigma$, less than that expected from one set of XRT data. We then analyzed only the first set of XRT data, for which the observation started 7.1 hr after the burst. Spectral response files were generated using the `xrtmkarf` task and the latest calibration database files (CALDB version 8, 2006-04-27).

As shown in figure 3, the X-ray light curve in the

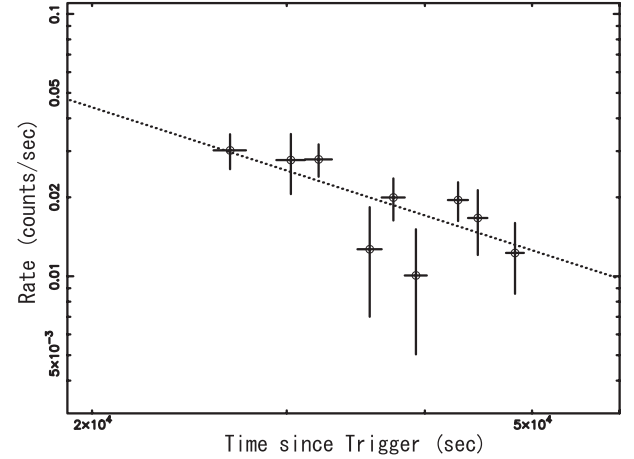


Fig. 3. X-ray light curve taken by *Swift*/XRT. The dashed line shows the best-fit power law function.

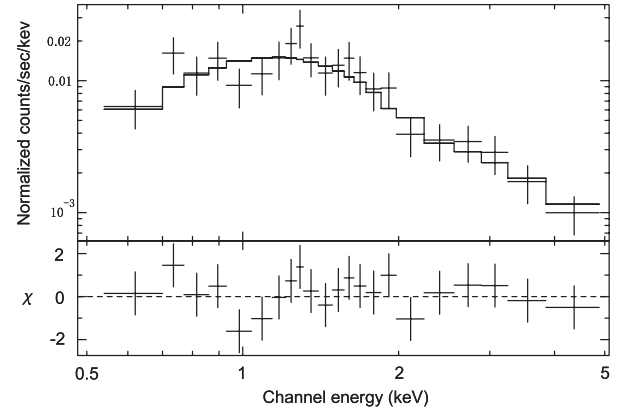


Fig. 4. X-ray spectrum taken by *Swift*/XRT. The spectrum is well fitted by the absorbed power law with a photon index of $\Gamma = 2.3^{+0.5}_{-0.4}$, and an absorbing column density of $N_{\text{H}} = 3.1^{+0.2}_{-0.1} \times 10^{22} \text{ cm}^{-2}$.

0.5–5.0 keV band is reasonably fit to a power-law model with $\alpha = -1.37 \pm 0.38$ and $\chi^2/\text{d.o.f.} = 1.00/7$, which is consistent with, or slightly steeper than, that of the optical value. The 0.5–5.0 keV spectrum (figure 4) is well fitted by an absorbed power law, where the photon index is $\Gamma = 2.3^{+0.5}_{-0.4}$ with an absorbing column of $N_{\text{H}} = 3.1^{+0.2}_{-0.1} \times 10^{22} \text{ cm}^{-2}$ and $\chi^2/\text{d.o.f.} = 0.67/19$. According to Dickey and Lockman (1990), the galactic column density of this line of sight is estimated to be $1.2 \times 10^{21} \text{ cm}^{-2}$. The mean flux during the observation is $1.08^{+0.24}_{-0.73} \times 10^{-12} \text{ erg cm}^{-2} \text{ s}^{-1}$, which is about 1 order fainter than those of optically bright GRB's X-ray afterglows, such as GRB 050319 (Cusumano et al. 2006), GRB 051111 (Butler et al. 2006), and GRB 060124 (Romano et al. 2006). These analyses of light curve and spectrum indicate that this X-ray afterglow behavior agrees with the standard model in terms of the relation between the temporal and spectral indices, assuming that we are observing a spherical fireball in a frequency range above that of synchrotron cooling (Sari et al. 1999).

³ (<http://heasarc.gsfc.nasa.gov/docs/software/lheasoft/>).

4. Discussion

LOT was used to detect the optically dim afterglow of GRB 051028. The brightness around 0.1 d after the burst was about 3 mag fainter than that of the dark GRB 020124 (Berger et al. 2002). The temporal evolution of the optical afterglow shows a plateau phase around 0.1 d after the burst. These features, with the exception of the brightness, resemble those of recent optically bright afterglows. The X-ray afterglow is also 1 order fainter than those of optically bright GRB's X-ray afterglow. In contrast with one typical, optically dark event, GRB 021211, the light curve of GRB 051028 shows the usual pattern of temporal decay, with an index of $\alpha = -0.904$. This is different from optically dark GRBs, which show rapid decay from very early phases, such as for GRB 021211.

The optical darkness of the GRB 051028 optical afterglow may instead be a result of high circumburst extinction. However, the column density, N_{H} , shows no significant excess over the Galactic value. The observed N_{H} (90% confidence level) is consistent with that of the Galactic value. Since this value is insufficient to explain the optical darkness of dark GRBs, the extinction model of optically dark GRBs is also not applicable to the present case. These results are supported by SCUBA observations of several dark GRBs; the sub-mm results suggest that the optically dark GRBs do not occur in particularly dusty environments (Barnard et al. 2003).

Although the redshift of GRB 051028 was not determined from optical spectroscopic observations, a value of pseudo- $z = 3.7 \pm 1.8$ can be derived for this burst using the pseudo- z estimator developed by Pelangeon et al. (2006). Even assuming the highest allowed redshift ($z = 5.5$), the Ly α line and continuum absorption is expected to affect the R -band flux of the afterglow by only ~ 2 mag. In this calculation, the optical depth was calculated following Yoshii and Peterson (1994), and the spectral index, as computed from the X-ray afterglow, was fixed at $\beta = -1.3$. This calculation also successfully explains the drop in the B band in the spectra of the GRB 050319 ($z = 3.24$) afterglow (Huang et al. 2007). Since the expected R -band absorption is not high enough to explain the darkness of the afterglow, it is inappropriate to use the high- z scenario for optically dark GRBs, at least for the particular case of GRB 051028. The afterglow spectral index, β_{ox} , at 11 hr after the burst derived from X-ray and optical data is also a useful indicator of the optical darkness as Jakobsson et al. (2004). For the current event, the index $\beta_{\text{ox}} \sim -0.6$ agrees with the standard afterglow model and implies that the optical darkness is unlikely to support high- z and obscuration.

The above discussion suggests that the brightness of the GRB 051028 afterglow is intrinsically optically dark, although the prompt fluence is brighter than that of optically bright events, such as GRB 021004. The brightness of X-ray afterglow also supports this hypothesis. Figure 5 shows the R -band brightness at 0.1 d against the prompt fluence. It can be seen that they have the same redshift range as does GRB 051028 ($z = 3.7 \pm 1.8$) detected by HETE-2. This result implies that the afterglow emission mechanism or the energy conversion to the afterglows may be the origin of the darkness. Swift formulated the canonical X-ray afterglow behavior, which led to the observation of early optical afterglows. These

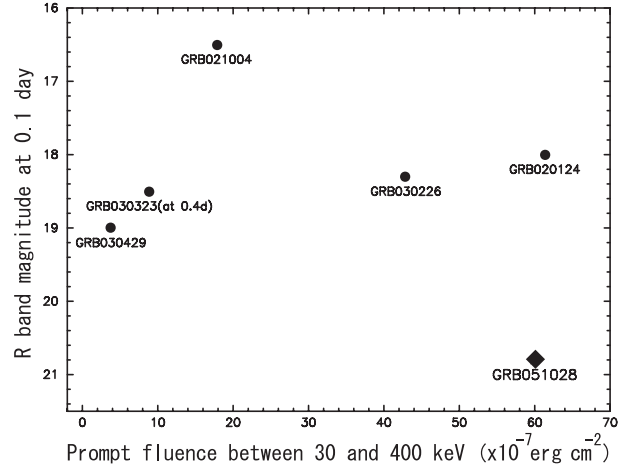


Fig. 5. Brightness in the R -band at 0.1 d after the burst plotted against the prompt fluence between 30 and 400 keV. The prompt fluence comes from Hurley et al. (2005) for GRB 051028 and Sakamoto et al. (2005) for others.

X-ray and optical light curves show rapid and shallow decay in the early phase. These various variabilities may be explained by the standard forward shock scenario, with some additional components, such as continuous activities related to the central engine, energy injection, patch shell, and 2 jet models (e.g., Ioka et al. 2005). The $t < 0.1$ d plateau phase of GRB 051028 could be explained by energy injection within the context of a forward shock model. In a case of less energy input, there are two expected features: (1) the brightness of the optical afterglow will be dim, and (2) the temporal behavior will have a shorter shallow decay phase than those of bright afterglows, which is similar to the pure standard model. The shallow decay period of the current GRB 051028 is obviously less than that of the bright afterglow. While the bright event of GRB 050319 has a longer shallow decay phase (~ 1 d), the afterglow of GRB 051028 shows the classical temporal decay pattern ($\alpha = -0.9$) from 0.1 d after the burst.

5. Conclusion

We made optical observations using both WIDGET and the Lulin 1 m telescope. Based on our optical follow-up observation, it can be seen that the optical afterglow shows a possible plateau phase at 0.1 d, which is similar in behavior, but not in brightness, to optically bright afterglows (e.g., GRB 041006, Urata et al. 2007; GRB 050319, Huang et al. 2007). The brightness is 3 mag fainter than that of the optically dark GRB 020124. The X-ray spectrum analysis implies that there is no significant extinction by the host galaxy. Furthermore, according to a model calculation of the Ly α absorption limit of GRB 051028's redshift, the expected R -band absorption is not high enough to explain the darkness of the afterglow. These arguments indicate that the faintness of the afterglow of GRB 051028, that is the optical darkness of the burst, is not due to its being obscured by dust, but because it is intrinsically dim.

We thank all staff and observers of the Lulin telescope for various arrangements in realizing this observation. This

work is supported by NSC 93-2752-M-008-001-PAE and NSC 93-2112-M-008-006. Y. U. acknowledges support from Japan Society for the Promotion of Science (JSPS) through JSPS Research Fellowships for Young Scientists.

References

- Barnard, V. E., et al. 2003, MNRAS, 338, 1
Berger, E., et al. 2002, ApJ, 581, 981
Butler, N. R., et al. 2006, ApJ, 652, 1390
Castro-Tirado, A. J., et al. 2006, A&A, 459, 763
Crew, G. B., et al. 2003, ApJ, 599, 387
Cusumano, G., et al. 2006, ApJ, 639, 316
Dickey, J. M., & Lockman, F. J. 1990, ARA&A, 28, 215
Fynbo, J. U., et al. 2001, A&A, 369, 373
Heise, J. 2001 (astro-ph/0111246)
Henden, A. 2005, GRB Coord. Netw. Circ., 4184
Huang, K. Y., et al. 2005, Nuovo Cimento C, 28, 731
Huang, K. Y., et al. 2007, ApJ, 654, L25
Hurley, K., et al. 2005, GRB Coord. Netw. Circ., 4172
Ioka, K., Kobayashi, S., & Zhang, B. 2005, ApJ, 631, 429
Jakobsson, P., Hjorth, J., Fynbo, J. P. U., Watson, D., Pedersen, K., Björnsson, G., & Gorosabel, J. 2004, ApJ, 617, L21
Jelinek, M., et al. 2005, GRB Coord. Netw. Circ., 4175
Klose, S., et al. 2003, ApJ, 592, 1025
Lamb, D. Q., et al. 2003 (astro-ph/0310414)
Masuno, K., et al. 2006, GRB Coord. Netw. Circ., 5190
Pelangeon, A., et al. 2006 (astro-ph/0601150)
Piro, L., et al. 2002, ApJ, 577, 680
Racusin, J., Page, K., Kennea, J., Morris, D., Pagani, C., Burrows, D., & Gehrels, N. 2005, GRB Coord. Netw. Circ., 4174
Romano, P., et al. 2006, A&A, 456, 917
Sakamoto, T., et al. 2005, ApJ, 629, 311
Sari, R., Piran, T., & Halpern, J. P. 1999, ApJ, 519, L17
Shirasaki, Y., et al. 2003, PASJ, 55, 1033
Tamagawa, T., et al. 2005, Nuovo Cimento C, 28, 771
Urata, Y., et al. 2005, Nuovo Cimento C, 28, 775
Urata, Y., et al. 2007a, ApJ, 655, L81
Urata, Y., et al. 2007b, ApJ submitted
Yamazaki, R., Ioka, K., & Nakamura, T. 2003, ApJ, 593, 941
Yoshii, Y., & Peterson, B. A. 1994, ApJ, 436, 551